Constraint method for deriving nonequilibrium molecular dynamics equations of motion

T. M. Galea and Phil Attard
Ian Wark Research Institute, University of South Australia, Mawson Lakes, South Australia 5095, Australia
(Received 23 July 2002; published 24 October 2002)

A procedure for developing non-Hamiltonian equations of motion for constrained systems is given. It is shown that such constraints can be used to mimic common statistical systems, both equilibrium (e.g., constant temperature) and nonequilibrium (e.g., shear flow, heat flow), and the procedure is suited for molecular dynamics computer simulations. The method is demonstrated with isokinetic shear flow, in bulk and slit geometries, which illustrates its flexibility. Results for the shear viscosity are in agreement with previously published results.

DOI: 10.1103/PhysRevE.66.041207 PACS number(s): 66.20.+d, 02.70.Ns, 61.20.Ja, 61.20.Lc

I. INTRODUCTION

Molecular dynamics computer simulations are being used to describe increasingly complex systems [1]. Originally restricted to a constant energy isolated system (microcanonical system) molecular dynamics has since been used for constant temperature [2] and constant pressure [3] equilibrium systems, as well as in a variety of nonequilibrium applications [4]. Such embellishments necessarily invoke non-Hamiltonian equations of motion, and this raises fundamental questions about the status of the approaches and the nature of the statistical distribution generated by the consequent trajectory. Further, the equations of motion tend to be *ad hoc* in the sense that they are developed specifically for the problem at hand, and there appears no fundamental principle that can be used to judge between alternative equations of motion or any systematic procedure that can be used to develop equations for new systems.

This paper treats a generic class of systems that are constrained in some sense, and develops appropriate equations of motion by invoking a geometrical principle of least constraint. The utility of this class is that many thermodynamic systems, both equilibrium and nonequilibrium, may be mimicked by invoking constraints on macroscopic variables. For example, a constant temperature system can be modeled as one with fixed kinetic energy, which leads to the isokinetic thermostat [4–6]. Poiseuille flow can be represented by a system with constant total momentum for the confined fluid and zero momentum for the walls. Couette flow can be obtained by constraining the momentum in two halves of the system to be constant and equal and opposite. There is a wide variety of systems that can be cast as constrained, and the present principle for developing non-Hamiltonian equations of motion for such systems provides a systematic and unified approach to the problem.

The paper is divided into two parts. Section I derives the equations of motion for an arbitrary constraint and for a general phase space metric. The equivalence of the so-called projected metric with Gauss's principle of least constraint is shown, and the implementation of the method for a discrete time step is also discussed. Section II gives equations of motion for shear flow by invoking a constraint on the momenta in the two halves of the system. Results are given for bulk and for confined Lennard-Jones fluids and it is shown that the shear viscosity obtained with the method is in agreement with literature values.

II. PRINCIPLE OF LEAST CONSTRAINT

A. Equations of motion

Denote the position of the ith particle by $\mathbf{q}_i$ and its momentum by $\mathbf{p}_i$, so that a point in $6N$-dimensional phase space is $\mathbf{\Gamma}=(\mathbf{q}^N,\mathbf{p}^N)$, and the trajectory of the system is $\mathbf{\Gamma}(t)$. Suppose that the system is subject to a constraint, the general form of which is

$$g(\mathbf{q}^N,\mathbf{p}^N,t)=G, \tag{1}$$

where G is a constant. The equations of motion for the constrained system may be written as

$$\dot{\mathbf{q}}_i=\frac{\partial\mathcal{H}}{\partial\mathbf{p}_i}+\lambda\nabla_{\mathbf{q}i}g=\dot{\mathbf{q}}_i^0+\lambda\nabla_{\mathbf{q}i}g,$$

$$\dot{\mathbf{p}}_i=-\frac{\partial\mathcal{H}}{\partial\mathbf{q}_i}+\lambda\nabla_{\mathbf{p}i}g=\dot{\mathbf{p}}_i^0+\lambda\nabla_{\mathbf{p}i}g, \tag{2}$$

where $\mathcal{H}(\mathbf{\Gamma})$ is the Hamiltonian. The first terms on the right hand side represent the natural or unconstrained motion of the system, and the second term represents a generalized force of constraint. The constraint force is directed along the gradient to the hypersurface and as such is minimal in a least squares metrical sense. The multiplier λ is determined by the vanishing of the time derivative of the constraint,

$$\dot{g}=\frac{\partial g}{\partial t}+\dot{\mathbf{\Gamma}}\cdot\nabla g=0. \tag{3}$$

Implicit in the above equations is the metric of phase space. One can define constant length elements l_{qi} and l_{pi} such that scalar products have the form

$$\mathbf{\Gamma}^{(1)}\cdot\mathbf{\Gamma}^{(2)}=\sum_{i\alpha}\left[\frac{1}{l_{qi}^2}q_{i\alpha}^{(1)}q_{i\alpha}^{(2)}+\frac{1}{l_{pi}^2}p_{i\alpha}^{(1)}p_{i\alpha}^{(2)}\right], \tag{4}$$

where $\alpha=x$, y, or z, and gradients have the form

$$\nabla f(\mathbf{\Gamma}) = \sum_i \left[l_{qi}^2 \frac{\partial f}{\partial \mathbf{q}_i} \hat{\mathbf{q}}_i + l_{pi}^2 \frac{\partial f}{\partial \mathbf{p}_i} \hat{\mathbf{p}}_i \right]. \tag{5}$$

The product of the lengths has no physical consequence, and without loss of generality it can be set equal to unity, $l_{qi} l_{pi} = 1$. (Alternatively, the product could be set equal to Planck's constant.) It is the ratio of the two lengths that is crucial (this determines the relative importance of position and momentum), and this must have the dimensions of mass divided by time, $l_{pi}/l_{qi} = m_i/\tau$. Accordingly one has

$$l_{qi}^2 = \frac{\tau}{m_i}, \quad l_{pi}^2 = \frac{m_i}{\tau}. \tag{6}$$

The time scale τ affects the direction in phase space of the gradient to the hypersurface, but there does not appear to be any general argument to fix its value. However, it does appear that the physical value corresponds to $\tau \to 0$; this limit will be taken shortly.

With these expressions for the length scales in phase space, the equations of motion explicitly are

$$\dot{q}_{i\alpha} = \frac{\partial \mathcal{H}}{\partial p_{i\alpha}} + \lambda \frac{\tau}{m_i} \frac{\partial g}{\partial q_{i\alpha}},$$

$$\dot{p}_{i\alpha} = -\frac{\partial \mathcal{H}}{\partial q_{i\alpha}} + \lambda \frac{m_i}{\tau} \frac{\partial g}{\partial p_{i\alpha}}, \tag{7}$$

and the distance moved along the gradient is

$$\lambda = \left\{ -\frac{\partial g}{\partial t} - \sum_{i\alpha} \left[\frac{\partial \mathcal{H}}{\partial p_{i\alpha}} \frac{\partial g}{\partial q_{i\alpha}} - \frac{\partial \mathcal{H}}{\partial q_{i\alpha}} \frac{\partial g}{\partial p_{i\alpha}} \right] \right\} \Bigg/ \sum_{i\alpha} \left[\frac{\tau}{m_i} \left(\frac{\partial g}{\partial q_{i\alpha}} \right)^2 + \frac{m_i}{\tau} \left(\frac{\partial g}{\partial p_{i\alpha}} \right)^2 \right]. \tag{8}$$

In these general equations of motion, the forces of constraint contribute to the velocities as well as to the accelerations, which is arguably unphysical. This can be rectified by taking the limit $\tau \to 0$, in which case the equations of motion become

$$\dot{q}_{i\alpha} = \frac{\partial \mathcal{H}}{\partial p_{i\alpha}},$$

$$\dot{p}_{i\alpha} = -\frac{\partial \mathcal{H}}{\partial q_{i\alpha}} + \lambda' m_i \frac{\partial g}{\partial p_{i\alpha}}, \tag{9}$$

and the distance factor is now

$$\lambda' = \left\{ -\frac{\partial g}{\partial t} - \sum_{i\alpha} \left[\frac{\partial \mathcal{H}}{\partial p_{i\alpha}} \frac{\partial g}{\partial q_{i\alpha}} - \frac{\partial \mathcal{H}}{\partial q_{i\alpha}} \frac{\partial g}{\partial p_{i\alpha}} \right] \right\} \Bigg/ \sum_{i\alpha} m_i \left(\frac{\partial g}{\partial p_{i\alpha}} \right)^2. \tag{10}$$

This $\tau \to 0$ limit may be called the projected metric (because it measures the length of a vector from its projection onto the hyperplane of momenta).

B. Gauss's principle

The equations of motion that have the least force of constraint in the projected metric may also be derived from Gauss's principle of least constraint. This is based upon minimization of the Hertzian curvature [4]

$$C = \frac{1}{2} \sum_{i\alpha} \frac{1}{m_i} \left(\dot{p}_{i\alpha} + \frac{\partial \mathcal{H}}{\partial q_{i\alpha}} \right)^2 \tag{11}$$

with respect to acceleration, subject to the constraint (3). Introducing a Lagrange multiplier, one has

$$0 = \frac{\partial (C - \lambda' \dot{g})}{\partial \dot{p}_{i\alpha}} = \frac{1}{m_i} \dot{p}_{i\alpha} + \frac{1}{m_i} \frac{\partial \mathcal{H}}{\partial q_{i\alpha}} - \lambda' \frac{\partial g}{\partial p_{i\alpha}}. \tag{12}$$

This is identical to the projected metric result, Eq. (9).

C. Discrete time step

Molecular dynamics computer simulations necessarily invoke a discrete time step of non-zero length. Whilst there exist methods to solve the equations of motion to high accuracy, some numerical error is inevitable. Unfortunately, because the constraint enters as a time derivative, there is no means to correct for system drift away from the hypersurface of constraint. For example, the Gaussian thermostat based upon the isokinetic constraint is usually supplemented with periodic rescaling of velocities to correct for the drift in the kinetic temperature [1]. This rescaling is both *ad hoc* and artificial and it is preferable to avoid it.

Simplectic integrators have proven efficient in minimizing drift [7]. An alternative approach in the present formalism for the discrete case is to allow the system to evolve from the point $\mathbf{\Gamma}(t)$ to the point $\mathbf{\Gamma}^{(0)}$ at time $t + \Delta_t$. This evolution can be either the pure Hamiltonian natural evolution or the constrained evolution, and the equations of motion can be solved to as high accuracy as desired. In either case $\mathbf{\Gamma}^{(0)}$ will not be exactly on the constraint hypersurface. However, one can move the trajectory back to the closest point on the hypersurface by calculating successively

$$\lambda^{(n)} = \frac{G - g(\mathbf{\Gamma}^{(n-1)})}{\nabla g \cdot \nabla g^{(n-1)}} \tag{13}$$

and

$$\mathbf{\Gamma}^{(n)} = \mathbf{\Gamma}^{(n-1)} + \lambda^{(n)} \nabla g. \tag{14}$$

Here the gradient of the hypersurface can be evaluated at any convenient point (e.g., $\mathbf{\Gamma}^{(n-1)}$), and the appropriate metric lengths should be used. After n iterations, when the trajectory is back on the hypersurface within some specified tolerance, one simply sets $\mathbf{\Gamma}(t + \Delta_t) = \mathbf{\Gamma}^{(n)}$. This method precludes drift away from the hypersurface and avoids the need for periodic rescaling or other *ad hoc* moves to make the system satisfy the constraints.

For the case of multiple constraints, $g_a(\mathbf{\Gamma}) = G_a$, $a = 1,2,\ldots,$ one has to solve the linear system of equations

$$\sum_b \lambda_b^{(n)} \nabla g_b \cdot \nabla g_a^{(n-1)} = G_a - g_a^{(n-1)}, \quad a = 1,2, \ldots \quad (15)$$

for the $\lambda^{(n)}$. The nth estimate for the trajectory is

$$\mathbf{\Gamma}^{(n)} = \mathbf{\Gamma}^{(n-1)} + \sum_a \lambda_a^{(n)} \nabla g_a . \quad (16)$$

III. AN EXAMPLE: ISOKINETIC SHEAR FLOW

A. Review

As mentioned in the Introduction, constant temperature molecular dynamics have previously been performed using the so-called Gaussian thermostat, which constrains the kinetic energy [4–6]. Other constant temperature molecular dynamics methods include the Nosé-Hoover thermostat [2,8,9] and stochastic methods that yield the Boltzmann distribution [3,10,11].

The shear viscosity has been obtained by equilibrium molecular dynamics simulations using the Green-Kubo method [12,13]. Nonequilibrium methods include driven flow with a sinusoidal profile [14], trajectory perturbation methods [15], boundary driven flow [16], including sliding brick boundary conditions [17], and modified equations of motion such as the DOLLS tensor [13] and the SLLOD equations (so named because of its close relationship to the DOLLS tensor algorithm) [18,19]. Extensive results for the shear viscosity of a Lennard-Jones fluid at its triple point exist in the literature [12,16,20–27].

B. Constraints

Constrained equations of motion will now be developed for shear flow, $v_x = \gamma y$, where γ is the shear rate. It remains to specify an appropriate constraint.

One possibility would be to fix the momentum of each particle according to its position, $p_{ix} = m\gamma q_{iy}$. However, this is a very strong constraint that does not allow fluctuations about the average velocity profile. Nor does it allow nonlinear profiles to develop. What is required is the least constraint that can be imposed to cause shear flow, an idea that is consistent with, but distinct from, the idea of the least constraint force in the equations of motion.

The constraint chosen here is that the total momentum in the top half of the system is fixed, and equal and opposite to that in the bottom half of the system. That is, two constraint functions are defined,

$$g_\pm(\mathbf{\Gamma}) \equiv \sum_{i=1}^{N} p_{ix} \Theta(\pm q_{iy}), \quad (17)$$

where Θ is the Heaviside step function. In order to achieve a shear rate γ, one can see that the value of the constrained momenta should be

$$g_\pm(\mathbf{\Gamma}) = \frac{\pm \gamma L N m}{8} \equiv \pm G, \quad (18)$$

where L is the height of the simulation cell, m is the particle mass, and N is the number of particles. The requisite derivatives of the momentum hypersurfaces are

$$\frac{\partial g_\pm}{\partial q_{i\alpha}} = \pm p_{ix} \delta(q_{iy}) \delta_{\alpha y}, \quad \frac{\partial g_\pm}{\partial p_{i\alpha}} = \Theta(\pm q_{iy}) \delta_{\alpha x}, \quad (19)$$

where Kronecker and Dirac delta functions appear. The Dirac δ arises from a particle crossing the midplane, and it only contributes to the time derivatives when a particle is precisely at the midplane. In a finite-sized simulation the probability that this occurs is negligible, and henceforth this term will be ignored.

The shear causes the system to heat up, and so an isokinetic constraint is also imposed to maintain the desired temperature. The peculiar kinetic energy is

$$k(\mathbf{\Gamma}) \equiv \frac{1}{2m} \sum_{i=1}^{N} \tilde{\mathbf{p}}_i \cdot \tilde{\mathbf{p}}_i , \quad (20)$$

where the peculiar momentum is measured with respect to the local velocity profile $\tilde{\mathbf{p}}_i = \mathbf{p}_i - m\gamma q_{iy} \hat{\mathbf{p}}_{ix}$. By the equipartition theorem, the value of the constrained peculiar kinetic energy is

$$k(\mathbf{\Gamma}) = \frac{3Nk_BT}{2} \equiv K, \quad (21)$$

where k_B is the Boltzmann's constant and T is the temperature. The derivatives of the kinetic energy hypersurface are

$$\frac{\partial k}{\partial q_{i\alpha}} = -\gamma \tilde{p}_{ix} \delta_{\alpha y}, \quad \frac{\partial k}{\partial p_{i\alpha}} = \frac{1}{m} \tilde{p}_{i\alpha} . \quad (22)$$

In view of these expressions, the constrained equations of motion are

$$\dot{q}_{i\alpha} = \frac{\partial \mathcal{H}}{\partial p_{i\alpha}} - \frac{\tau^2}{m} \lambda' \gamma \tilde{p}_{ix} \delta_{\alpha y}, \quad (23)$$

$$\dot{p}_{i\alpha} = \frac{-\partial \mathcal{H}}{\partial q_{i\alpha}} + m[\lambda'_+ \Theta(q_{iy}) \delta_{\alpha x} + \lambda'_- \Theta(-q_{iy}) \delta_{\alpha x} + \lambda' \tilde{p}_{i\alpha}/m]. \quad (24)$$

It is tedious but straightforward to show that the distances are

$$\lambda'_\pm = -\frac{\dot{p}_x^{0\pm} + \lambda' \tilde{p}_x^\pm}{mN_\pm} \quad (25)$$

and

$$\lambda' = \frac{mN_+N_-\dot{k}^0 - N_-\tilde{p}_x^+ \dot{p}_x^{0+} - N_+\tilde{p}_x^- \dot{p}_x^{0-}}{N_-(\tilde{p}_x^+)^2 + N_+(\tilde{p}_x^-)^2 - 2N_+N_-k}. \quad (26)$$

Here $N_\pm$ and $\tilde{p}_x^\pm$ are the number of atoms and the peculiar momentum in the respective halves of the system, and the natural rate of change of momentum and of peculiar kinetic

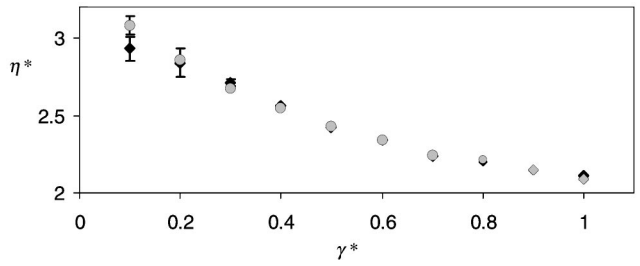

FIG. 1. Shear viscosity curve for a homogeneous system using the present geometric technique (gray circles), compared to the SLLOD results from Heyes (black diamonds) [25]. The standard error is indicated where the error bars are larger than the symbols.

energy are $\dot{p}_x^{0\pm}=\Sigma_i \dot{p}_{ix}^0 \Theta(\pm q_{iy})$ and $\dot{k}^0=\Sigma_{i\alpha}\tilde{p}_{i\alpha}[\dot{p}_{i\alpha}^0/m-\gamma \dot{q}_{iy}^0 \delta_{\alpha x}]$, respectively. Note that the constraint force acting on the rate of change of position is quadratic in the time scale τ, and that acting on the rate of change of momentum is independent of τ.

In the actual simulations, the discrete equations of motion for multiple constraints, Eqs (15) and (16), were used. The explicit formulas can be obtained using an analysis similar to the above. The equations were iterated successively until convergence. This iteration procedure guarantees that the system returns to the constraint hypersurface after each finite time step, and there was no need for the periodic velocity rescaling that is used with the usual implementation of the isokinetic method.

C. Simulation details and results

1. Homogeneous system

The geometric constraint technique for isokinetic shear flow was implemented in a homogeneous system using Lees-Edwards boundaries [17]. Argon at the triple point ($T=0.722\epsilon/k_B, \rho=0.8442\sigma^{-3}$) was chosen because there has been a large amount of data published for this system [12,16,20–27]. Here ϵ is the energy parameter and σ is the length parameter that appear in the Lennard-Jones pair potential. The central cell contained 125 atoms. For shear rates of $\gamma^*=0.5,\ldots,1$, where $\gamma^*=\gamma(m\sigma^2/\epsilon)^{1/2}$, simulations were run for 200 000 steps with an integration time step of $\Delta t^*=0.0015$, where $\Delta t^*=\Delta t(\epsilon/m\sigma^2)^{1/2}$. For shear rates of $\gamma^*=0.1,\ldots,0.4$, simulations were run for 400 000 steps with a time step $\Delta t^*=0.0024$. A fifth-order Gear predictor-corrector scheme was used, and excellent agreement with past results was obtained for the shear viscosity. Below they are compared with the results of Heyes [25], who used the SLLOD equations of motion with Lees-Edwards boundaries and a Gaussian isokinetic thermostat. The viscosity was determined in the usual manner from the ratio of the stress tensor to the shear rate. The dimensionless viscosity is $\eta^*=\eta\sigma^2/(m\epsilon)^{1/2}$.

The momentum constraints, in combination with the Lees-Edwards boundary conditions and the isokinetic thermostat on the peculiar momentum, were found to produce a linear velocity profile with the desired shear rate. It can be seen from Fig. 1 that the shear thinning at high shear rates is correctly captured by the present method. For shear rates $\gamma^*>0.1$, the results are in extremely good agreement with Heyes [25]. The larger error at low shear, which is commonly observed, is due to the low signal to noise ratio at such low shear rates. The large viscosity gradient at low shear rates also contributes to this error, because any errors or fluctuations in the shear rate will cause a correspondingly large variation in viscosity. The agreement of these results with those previously published for the SLLOD case is promising and indicates that the new equations of motion do not effect the flow adversely.

Only the ratio of the coordinate and momentum metric is significant, and from Eq. (6) this ratio is $l_q^2/l_p^2=\tau^2/m^2$. The time constant τ for the metric was taken as the time step Δt used in the computer implementation of the constraint equations. That is, $\tau^*=0.0015$ for $\gamma^*<0.4$. In practice this natural metric based on molecular parameters is effectively the projected metric mentioned previously because there is virtually no change to the positions due to the constraint force. To investigate the effect of changing the metric, simulations were carried out with τ^* multiplied by a factor of 10^{28}. This caused a change in the positions in the fifth decimal place for a shear rate of $\gamma^*=1$. Any multiplier larger than this eventually caused the coordinates to change too greatly and to produce an unsatisfactory energy due to particle overlap. This shows that a large change in the natural metric is required to move away from the projected metric. The viscosity for this nonprojected metric for shear rates $\gamma^*=0.1,\ldots,0.4$ is in very good agreement with the natural metric results, changing by less than 3% in each case.

The advantage of the constraint technique is that the system returns to the constant temperature and momentum (for each half) hypersurface for every time step. This was observed in practice, the temperature and the total momentum in each half remained constant and at the initially chosen value throughout the simulation. Velocity rescaling was never required. One may conclude that this constraint technique for finite time steps is a viable alternative to the continuum Gaussian thermostat as a temperature control method.

2. Inhomogeneous system

The results in Fig. 1 do not provide an unambiguous test of the constraint method for shear flow. It is well known that Lees-Edwards periodic boundaries alone have the ability to produce homogeneous shear and the peculiar definition of velocity required for temperature control (biased thermostat) also influences momentum flow [28]. So whilst the new equations cause no evident damage, because of these additional effects it cannot be concluded that the new equations themselves are producing the shear flow.

To determine whether the geometric method has the ability to produce shear flow independently of Lees-Edwards boundaries, these boundaries were removed and replaced with uniform walls in the xz plane. The wall potential was $v(y)=4\epsilon(\sigma/\zeta)^{12}$, where ζ is the distance of the center of the atom from the wall. This is the repulsive part of the Lennard-Jones potential, and it prevents atoms from leaving the simulation cell. The wall position was located at a distance $\rho^{-1/3}$

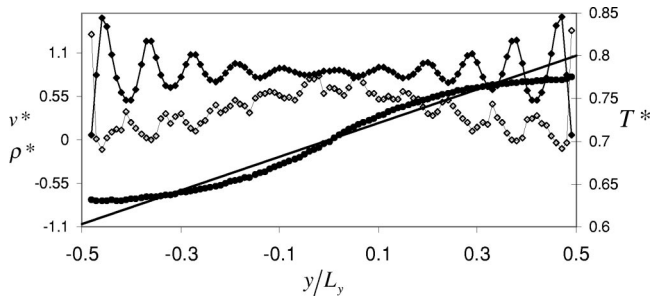

FIG. 2. Schematic of the potential wall system for a shear rate of 0.2, showing nonlinear density (solid diamonds), velocity (solid circles), idealized velocity (straight line), and the local temperature (open diamonds).

beyond the two boundaries at $y=\pm L/2$. This value was chosen so that the density of atoms in the simulation cell was close to the triple point density of argon. The periodic boundaries in the x and z direction remain unchanged. A cubic cell was used. Simulations were run for 200 000 steps, with a time step of $\Delta t^*=0.0024$, for 1000 particles.

To remove the effect of the profile-biased thermostat, the peculiar momentum of particles was based on the measured velocity profile in the shear direction (unbiased local thermostat) [28]. This also allows the effects of inhomogeneity and confinement on nonlinear velocity profiles to be explored.

As Fig. 2 shows, the resulting density profile is oscillating, which indicates a degree of ordering of the liquid into layers parallel to the plane of the potential boundary. This is a property of liquids confined between molecularly smooth solid boundaries [29], as was confirmed here by comparison with the prominent ordering observed in an equilibrium simulation that was also conducted. The velocity profile in Fig. 2 in the direction of the velocity gradient was nonlinear, with the gradient vanishing at the walls. The homogeneous velocity gradient for the same shear is also shown. The constraint guarantees that the area between the two velocity curves above the linear curve must equal that below the linear curve. This along with the vanishing of the gradient of the velocity profile at the walls results in a sharper gradient in the center. There was no correlation of the local velocity with the oscillating density profile.

It is expected that the nonuniformity in the velocity gradient is a phenomenon of the stationary smooth wall rather than the geometric equations of motion. The present potential wall corresponds to a completely nonwetting interface, and so complete slip could be expected. This is likely to be the cause of the vanishing of the velocity gradient at the boundary, due to the absence of any interaction with wall atoms. Such a lack of atomic interactions prevents the shearing of the fluid atoms near the boundary.

Interestingly the temperature profile is parabolic, being higher in the center by around 10%. This can be explained by larger heat production caused by the higher shear rate in the central region (the larger velocity gradient shown in Fig. 2). The heat is removed at an equal rate over the simulation cell by using a single Lagrange multiplier throughout, and so the central region is too hot, and the perimeter is too cold, as compared to the nominal temperature of $T^*=0.722$.

The slip behavior between the wall and the fluid atoms is a natural phenomenon observed in confined systems, both experimentally [30–32] and in computer simulations [33–35]. The present nonlinear velocity profile is an extreme example of such slippage, and it is a strength of the method that the geometric equations allow such a nonlinear profile to develop in this system. It would be difficult to realize this situation physically (because ordinarily shear flow is driven by the boundaries, and it would require a spatially inhomogeneous body force acting on the fluid to cause the present flow). Nevertheless, given shear flow and the noninteracting boundaries, such a nonlinear profile is realistic. The present approach shows the behavior of the fluid and the form of the slippage for this model flow.

A linear region was observed in the center of the cell for shear rates $\gamma^*<0.5$. Using the stress tensor, the shear rate and viscosity were calculated in this linear region, and the results are shown in Table I. The value of the shear viscosity deduced for the inhomogeneous system agrees well with that obtained for the homogeneous system discussed above (Fig. 1). This confirms that the fluid is behaving as expected and that the equations of motion are producing the correct fluid response under the present conditions.

The flexibility of the constraint technique allows alternative implementations of the isokinetic shear flow equations. One possibility is to constrain the momentum of the fluid in a region at the outer edges of the simulation cell only, thereby shearing the intervening fluid. Each of the two constrained fluid regions was set at approximately one molecular

TABLE I. Viscosity given by SLLOD [25], compared with that obtained here for the homogeneous system with the natural and the exaggerated metric, and with the results from the two inhomogeneous systems, the potential wall, and the constrained fluid boundary. Here γ^* is the nominal shear rate and γ_m^* is the measured shear rate in the center. The error in the last digit is given in the parentheses.

SLLOD [25]		Homogeneous		Wall		Constrained boundary	
		$\tau=\Delta t$	$\tau=10^{28}\Delta t$				
γ^*	η^*	η^*	η^*	γ_m^*	η^*	γ_m^*	η^*
0.1	2.93(8)	3.08(27)	3.17(9)			0.10	3.33(3)
0.2	2.84(9)	2.86(11)	2.91(7)			0.20	3.07(0)
0.3	2.71(2)	2.67(7)	2.67(3)	0.28	2.86(0)	0.30	2.80(0)
0.4	2.56(2)	2.54(8)	2.54(3)	0.44	2.40(0)	0.40	2.64(0)
0.5	2.42(1)	2.43(7)	2.44(2)			0.51	2.46(1)

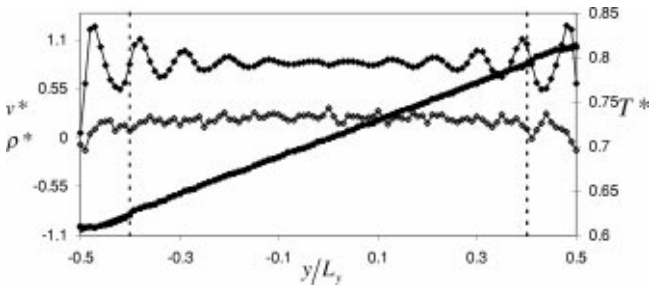

FIG. 3. Results for the boundary driven system for a shear rate of 0.2, showing density (solid diamonds), velocity (solid circles), idealized velocity profile (straight line, obscured), and the temperature (open diamonds). Dashed vertical lines represent the boundary of the constrained fluid region.

diameter, or 10% of the cell. This is similar to the fluid-wall method of Ashurst and Hoover [16]. However in the present case, fluid atoms are allowed to mix with the constrained fluid, in contrast to the method of Ashurst and Hoover where continuity is broken with an elastically reflecting boundary at the interface of the fluid and the fluid wall. An oscillating density profile is apparent again, as Fig. 3 shows. (Note that the uniform wall potential discussed in conjunction with the preceding figure was also present.) The velocity profile is nonlinear only in the constrained boundary region, with the velocity gradient vanishing at the wall once again. The velocity profile in the nonconstrained region is quite linear, and the actual shear rate is close to the ideal shear rate set by the boundaries. The viscosity obtained for boundary shear rates of 0.1–0.5 are shown in Table I. It can be seen that the results are again in close agreement with the homogeneous results, which confirms the reliability of the equations of motion that result from the geometric principle of least constraint, and the flexibility of the constrained macroscopic variable approach.

IV. DISCUSSION

In developing non-Hamiltonian equations of motion to describe different thermodynamic systems, it is desirable to perturb the natural motion of the system as little as possible. This requirement was implemented in the present paper in two ways. First a geometric principle of least constraint was analyzed. This gave the minimal additional force necessary to restrict the motion in phase space to a given constraint hypersurface. Results were given for both a general metric and a projected metric. The latter, it was argued, was the physically relevant case because the forces of constraint were projected onto the momentum hyperplane, as one would expect for real forces. In this case the geometrical principle became equivalent to Gauss's principle of least constraint. Using the molecular measure of time was found to be practically equivalent to the projected metric.

Second, the constraints that were imposed were also minimal. In the case of shear flow, two constraints were imposed. These fixed the total momentum in each half of the system to be equal and opposite, which is obviously much less restrictive than, for example, fixing the momentum everywhere. It was shown that a variety of flow patterns could develop, consistent with these two constraints. The general approach of constraining macroscopic conserved variables in different regions appears to offer the minimal solution to a variety of different nonequilibrium flows.

Specific results for shear flow were obtained to illustrate the present approach. The homogeneous results indicate that the supplementary forces from the geometric technique are not disturbing the system. The inhomogeneous methods show that the technique alone is capable of producing shear flow within the system. This technique also allows nonlinear velocity profiles to develop when they might not have been anticipated beforehand (e.g., the present results for the fluid confined by a potential wall). Advantages of the present method over other techniques are the following.

(1) The velocity profile is not assumed.

(2) The constraints are satisfied exactly at every time step and hence there is no need for velocity rescaling.

(3) There is minimal perturbation of the natural motion of the system.

(4) The technique is flexible, since it allows choice in the constraining factors, and the constraints may be applied to all or part of the fluid.

(5) The methods gives a well-defined and unambiguous recipe for developing equations of motion for different situations.

For the problem of homogeneous shear flow, the present method is of similar computational efficiency to the SLLOD equations and to the other nonequilibrium approaches to shear flow that are already in the literature [13–19]. The real advantage of the present approach is that it provides a first principles method for deriving equations of motion for general classes of flow. For example, momentum constraints could be used for Couette flow of complex fluids and for Poiseuille flow of confined fluids, and energy constraints could be used to simulate heat flow. The fact that the algorithm works in the present simple case of shear flow indicates that it can likely be applied more broadly.

[1] M.P. Allen and D.J. Tildesley, *Computer Simulation of Liquids* (Clarendon Press, Oxford, 1987).
[2] W.G. Hoover, Phys. Rev. A **31**, 1695 (1985)
[3] H.C. Andersen, J. Chem. Phys. **72**, 2384 (1980).
[4] W.G. Hoover, Annu. Rev. Phys. Chem. **34**, 103 (1983).
[5] W.G. Hoover, A.J.C. Ladd, and B. Moran, Phys. Rev. Lett. **48**, 1818 (1982).
[6] D.J. Evans, W.G. Hoover, B.H. Failor, B. Moran, and A.J.C. Ladd, Phys. Rev. A **28**, 1016 (1983).
[7] F. Zhang, D.J. Searles, D.J. Evans, J.S. den Toom Hansen, and D.J. Isbister, J. Chem. Phys. **111**, 18 (1999).
[8] S. Nosé, J. Chem. Phys. **81**, 511 (1984); Mol. Phys. **52**, 255 (1984).
[9] H.J.C. Berendsen, J.P.M. Potsma, W.F. van Gunsteren,

A. DiNola, and J.R. Haak, J. Chem. Phys. **81**, 3684 (1984).
[10] P. Attard, *Thermodynamics and Statistical Mechanics: Equilibrium by Entropy Maximisation* (Academic, London, 2002).
[11] P. Attard, J. Chem. Phys. **116**, 9616 (2002).
[12] D. Levesque, L. Verlet, and J. Kurkijarvi, Phys. Rev. A **7**, 1690 (1973).
[13] W.G. Hoover, D.J. Evans, R.B. Hickman, A.J.C. Ladd, W.T. Ashurst, and B. Moran, Phys. Rev. A **22**, 1690 (1980).
[14] E.M. Gosling, I.R. McDonald, and K. Singer, Mol. Phys. **26**, 1475 (1973).
[15] G. Ciccotti, G. Jacucci, and I.R. McDonald, Phys. Rev. A **13**, 426 (1976).
[16] W.T. Ashurst and W.G. Hoover, Phys. Rev. A **11**, 658 (1975).
[17] A.W. Lees and S.F. Edwards, J. Phys. C **5**, 1921 (1972).
[18] A.J.C. Ladd, Mol. Phys. **53**, 459 (1984).
[19] D.J. Evans and G.P. Morriss, Phys. Rev. A **30**, 1528 (1984).
[20] W.T. Ashurst, Phys. Rev. Lett. **31**, 206 (1973).
[21] W.T. Ashurst and W.G. Hoover, Phys. Lett. **61A**, 175 (1977).
[22] D.J. Evans, J. Stat. Phys. **22**, 81 (1980).
[23] D.J. Evans, Phys. Rev. A **23**, 1988 (1981).
[24] R. Bhupathiraju, P.T. Cummings, and H.D. Cochran, Mol. Phys. **48**, 1818 (1982).
[25] D.M. Heyes, J. Chem. Soc., Faraday Trans. 2 **82**, 1365 (1986).
[26] M.W. Evans and D.M. Heyes, Mol. Phys. **65**, 1441 (1988).
[27] D.P. Hansen and D.J. Evans, Mol. Simul. **13**, 375 (1994).
[28] D.J. Evans and G.P. Morriss, Phys. Rev. Lett. **56**, 2172 (1986).
[29] J.E. Lane and J.H. Spurling, Chem. Phys. Lett. **67**, 107 (1979).
[30] E. Bonaccurso, M. Kappl, and H.-J. Butt, Phys. Rev. Lett. **88**, 076103 (2002).
[31] U. Raviv, P. Laurat, and J. Klein, Nature (London) **413**, 51 (2001).
[32] V.S.J. Craig, C. Neto, and D.R.M. Williams, Phys. Rev. Lett. **87**, 054504 (2001).
[33] J.-L. Barrat and L. Bocquet, Phys. Rev. Lett. **82**, 4671 (1999).
[34] E. Manias, I. Bitsanis, G. Hadziioannou, and G. Tenbrinke, Europhys. Lett. **33**, 371 (1996).
[35] I. Bitsanis, J.J. Madga, M. Tirrell, and H.T. Davis, J. Chem. Phys. **87**, 1733 (1987).